

# Lateral patterning of nonlinear frequency conversion with transversely varying quasi-phase-matching gratings

G. Imeshev, M. Proctor, and M. M. Fejer

*E. L. Ginzton Laboratory, Stanford University, Stanford, California 94305*

Received January 6, 1998

We demonstrate control of the nonlinear conversion across a beam profile by using periodically poled lithium niobate with a laterally nonuniform quasi-phase-matching grating. As a representative experiment, generation of a flat-top second-harmonic beam is demonstrated. © 1998 Optical Society of America  
 OCIS codes: 190.2620, 050.2770, 140.0140, 160.3730.

The conversion in a nonlinear optical mixing process depends on the product of the pump field's amplitude and the interaction length, leading to inherently nonuniform conversion across the transverse profile of a Gaussian pump beam. This nonuniformity leads to several well-known problems such as back-conversion limitations on the dynamic range in second-harmonic generation<sup>1</sup> (SHG) and gain-induced diffraction in optical parametric amplification.<sup>2,3</sup> These effects limit conversion efficiency and can spoil the beam quality. To overcome the nonuniformity of nonlinear conversion in bulk devices one can use quadrature mixing,<sup>4</sup> but this method is complex to implement and leads to transversely varying polarization in the generated beam. In this Letter we describe an alternative method, based on the use of a laterally nonuniform quasi-phase-matching (QPM) grating to control the profile of the conversion transverse to the beam axis.

QPM is widely employed in frequency-conversion devices because it permits the use of noncritical phase matching and large nonlinear coefficients as well as provides wide spectral coverage.<sup>5</sup> In addition, QPM provides extra degrees of freedom in engineering the nonlinear properties of the medium, which are not available with conventional birefringent phase matching. For example, longitudinally aperiodic QPM gratings have been used to engineer the spectral dependence of the conversion,<sup>6-9</sup> and transverse variations of the period of a QPM grating have been used to provide a broad tuning range for SHG devices<sup>10</sup> and QPM optical parametric oscillators.<sup>11,12</sup> Here we discuss devices based on transverse variations in the length of the QPM grating.

Because the amplitude of a wave generated in a quasi-phase-matched mixing process depends on the length of the QPM grating, QPM with a transversely varying grating length can be used to engineer a desirable (such as uniform) conversion profile. In a region where there is no QPM grating, the mixing efficiency is negligible. Thus a QPM grating containing a region of unmodulated material whose length decreases with distance from the beam axis results in the effective interaction length's being shorter in the center and longer in the wings of the beam, resulting in a more uniform conversion across the beam (Fig. 1).

To discuss this process in more detail, we consider cw SHG as a prototypical example. If the SHG process is phase matched, the conversion efficiency  $\eta$  is<sup>1,13</sup>

$$\eta \equiv I_{2\omega}/I_{\omega} = \tanh^2(\sqrt{\eta_0}), \quad (1)$$

where  $I_{\omega}$  and  $I_{2\omega}$  are the pump and the second-harmonic (SH) intensities, respectively. The nonlinear drive,  $\eta_0$ , is defined as

$$\eta_0 = C^2 L^2 I_{\omega}, \quad (2)$$

where  $L$  is the interaction length and  $C$  is the material constant, defined by

$$C^2 = 8\pi^2 d_{\text{eff}}^2 / n_1^2 n_2 c \epsilon_0 \lambda^2, \quad (3)$$

where  $d_{\text{eff}}$  is the effective nonlinear coefficient,  $n_1$  and  $n_2$  are the refractive indices at the fundamental and the SH wavelengths, respectively,  $c$  is the speed of light, and  $\lambda$  is the fundamental wavelength. In the low conversion efficiency limit ( $\eta_0 \ll 1$ ), Eq. (1) reduces to

$$\eta = \eta_0, \quad (4)$$

so the drive can be recognized as the efficiency in the low conversion limit. Note, however, that at high drives the efficiency is a nonlinear function of  $\eta_0$ .

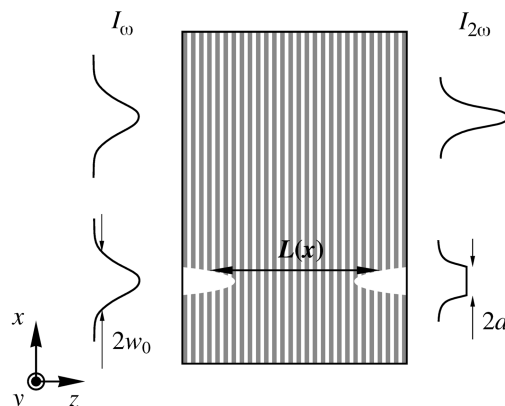


Fig. 1. Schematic comparison of uniform and nonuniform conversion for the SHG process.

An important quantity for bulk cw SHG is the power conversion efficiency  $\eta_P$ , defined as the ratio of the output power in the SH beam to the power input in the fundamental beam. Because the intensity of the pump beam is radially varying, the efficiency  $\eta$  is not uniform across the beam, so one can calculate  $\eta_P$  by averaging the conversion  $\eta$  over the radial distribution of the beams. This nonuniformity does not have serious implications in the low conversion limit, but as the conversion increases, the center of the beam is driven deeply into the saturated regime before the wings reach significant conversion. For example, for a Gaussian pump beam, obtaining a relatively modest  $\eta_P = 75\%$  requires a conversion efficiency of  $\eta = 96\%$  at the center of the beam, and the drive at the center of the beam must be  $\eta_0 = 5.1$ . At such high values of the nonlinear drive the acceptance bandwidth dramatically narrows,<sup>1</sup> leading to tight tolerances on phase-matching wavelength, temperature, and angular divergence. This effect is even more pronounced for pulsed SHG. The relevant efficiency is then the energy conversion efficiency  $\eta_E$ , defined as the ratio of the energy in the SH output pulse to the energy input in the pump pulse. If the intensity profile is Gaussian in both time and space and assuming that the pulses are long enough that the dispersion can be neglected, we find by integrating the conversion over space and time that to achieve  $\eta_E = 75\%$  the necessary peak conversion is 99% and the drive needed is 9.0.<sup>14</sup>

However, for cw SHG with a flat-top pump beam for which the intensity (and hence the drive) is radially constant across the beam, one can use a lower drive to obtain the same  $\eta_P$  than is required for cw SHG with a Gaussian beam. For such a flattened drive,  $\eta_P = \eta = 75\%$  is obtained at  $\eta_0 = 1.7$ . Although it is generally impractical to obtain flat-top pump beams, the drive can be made uniform across the central portion of a Gaussian pump beam by use of a radially varying QPM grating. According to Eq. (4), the drive is the small-signal conversion efficiency. To demonstrate engineering of the drive we designed a QPM grating such that the SH beam generated by a Gaussian pump beam would be truncated Gaussian (in one dimension), with a flat intensity profile over some range  $x \in [-a, a]$  (Fig. 1). Note that in this representative experiment we do not flatten the drive but rather generate a flat-top SH beam, a more extreme radial modification of the drive. We obtain the necessary condition on the drive by combining Eqs. (1) and (2):

$$I_\omega(x, y)\eta_0(x, y) = f(y), \quad x \in [-a, a], \quad (5)$$

where  $f(y)$  is a function that is independent of  $x$ . For a given pump beam profile the drive is controlled by the interaction length,  $L = L(x)$  [Eq. (2)], so for a Gaussian pump beam the functional form of the interaction length must be chosen as

$$L(x) = L_0 \begin{cases} \exp\left[\frac{2(x^2 - a^2)}{w_0^2}\right] & |x| \leq a, \\ 1 & |x| > a \end{cases} \quad (6)$$

where  $L_0$  is the physical length of the crystal and  $w_0$  is the  $1/e$  electric-field radius of the Gaussian pump beam. It should be noted here that the appropriate form of  $L(x)$  depends on the radius of the pump beam and the fraction of the beam over which the SH beam is to be flattened, so a particular grating design is appropriate only for a given pump beam. However, the absolute pump power affects the overall conversion but not the transverse dependence of the drive, so a particular design can be used over an arbitrary range of input powers. Because of the lithographically defined nature of the QPM structure, a grating with almost any desired shape of the unmodulated region can be fabricated, such as the one that satisfies Eq. (6). Clearly, this approach is valid for non-Gaussian pump beams as well, as long as their spatial profiles are sufficiently smooth and the focusing is loose enough that diffraction is not significant over the length of the interaction region.

Following the above design algorithm [Eq. (6)], we fabricated two patterned QPM gratings to generate flat-top SH beams truncated at  $a = \pm 0.50 w_0$  and  $a = \pm 0.75 w_0$ , with  $w_0 = 100 \mu\text{m}$ . The devices had length  $L_0 = 1 \text{ cm}$ , with unpatterned sections located symmetrically at both ends of the chips. We chose the QPM period of  $19 \mu\text{m}$  to achieve phase matching at  $20^\circ\text{C}$  for pumping at a fundamental wavelength of  $1.54 \mu\text{m}$ . The patterned periodically poled lithium niobate (PPLN) devices (Fig. 2) were fabricated from a 0.5-mm-thick  $\text{LiNbO}_3$  wafer according to the procedure described in Ref. 15.

The pump source was an Er:fiber laser that produced 5-mW cw output power at  $1.54 \mu\text{m}$ . The output Gaussian beam was focused to a spot size  $w_0 = 100 \mu\text{m}$  at the sample. The near field of the output SH beam was imaged onto a CCD camera. Figure 3 shows the intensity slices through the SH beams: (a) uniform grating SHG; (b) and (c) beams truncated at  $\pm 0.50 w_0$  and at  $\pm 0.75 w_0$ , respectively. These intensities were obtained from a single line of pixels along the  $x$  axis (as

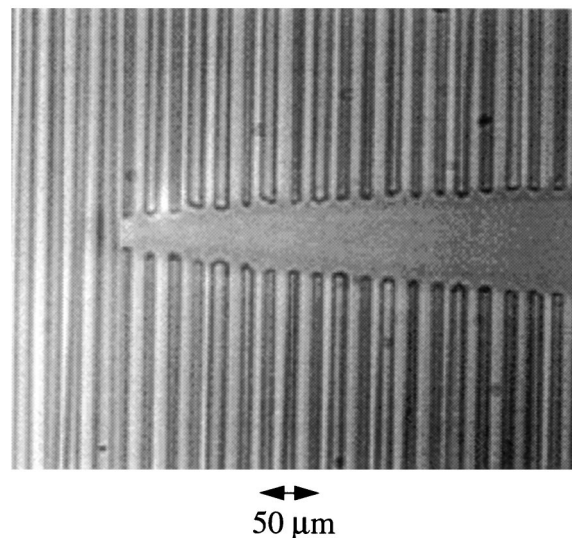


Fig. 2. Photograph of a portion of a 19- $\mu\text{m}$ -period PPLN chip, showing the pattern for generating the flat-top SH beam from a 100- $\mu\text{m}$ -radius Gaussian pump beam.

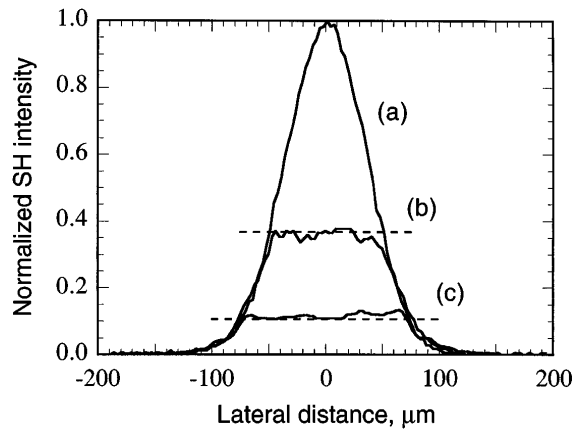


Fig. 3. Intensity slices through the generated SH beams: (a) uniform grating SHG; (b), (c) beams truncated at  $\pm 0.50w_0$  and at  $\pm 0.75w_0$ , respectively. Dashed lines indicate theoretical predictions for the flat portions of the truncated beams.

in Fig. 1) at the CCD camera, with no averaging over the  $y$  direction. The dashed lines indicate theoretical predictions for the flat portions of the truncated beams. The SH intensities along the  $y$  axis retain their Gaussian shape (not shown). It can be seen that the SH beam is flattened in one dimension, with the expected conversion efficiency.

In conclusion, we have described control of the nonlinear conversion across a beam profile by use of a QPM grating with transversely varying nonlinear interaction length. PPLN crystals with lithographically defined patterned QPM gratings were successfully fabricated and used to generate flat-topped SH beams from a Gaussian pump beam. An alternative approach to controlling the conversion across the pump beam is to use a QPM grating with transversely varying duty cycle. The duty cycle determines the effective nonlinear coefficient,<sup>5</sup> so patterning the duty cycle patterns the drive [Eqs. (2) and (3)]. The advantage of this method is that it alters only the amplitude but not the frequency dependence of the Fourier transform of the grating function. Hence, in contrast to a device with varying interaction length, this method preserves the tuning behavior of the device. Radial engineering of nonlinear conversion in two transverse dimensions can be accomplished in two steps by use of two crossed chips with the necessary rotation of polarization of both beams between the chips. Another method is to utilize a diffusion bonded stack of PPLN chips<sup>16</sup> with different unpoled patterns or duty cycle variation patterns, as would be suitable for high power pulsed optical parametric oscillators with large

apertures. Further directions of this research include applying transversely varying gratings to overcome nonuniform pump depletion and gain-induced diffraction in optical parametric generation and difference-frequency generation experiments. Also, the phase, rather than the amplitude, of the generated SH or parametric gain across a pump beam can be controlled by use of curved QPM gratings for control of transverse modes in resonator devices such as pulsed optical parametric oscillators.

This research was supported by the Defense Advanced Research Projects Agency under U.S. Office of Naval Research grant N00014-92-J-1903. M. Proctor was supported by the Swiss National Foundation of Scientific Research under grant 8220-040131. We thank Crystal Technology, Inc., for a generous donation of LiNbO<sub>3</sub> wafers.

## References

1. D. Eimerl, *IEEE J. Quantum Electron.* **QE-23**, 575 (1987).
2. S.-K. Choi, R.-D. Li, C. Kim, and P. Kumar, *J. Opt. Soc. Am. B* **14**, 1564 (1997).
3. C. Kim, R.-D. Li, and P. Kumar, *Opt. Lett.* **19**, 132 (1994).
4. D. Eimerl, *IEEE J. Quantum Electron.* **QE-23**, 1361 (1987).
5. M. M. Fejer, G. A. Magel, D. H. Jundt, and R. L. Byer, *IEEE J. Quantum Electron.* **28**, 2631 (1992).
6. M. A. Arbore, O. Marco, and M. M. Fejer, *Opt. Lett.* **22**, 865 (1997).
7. M. A. Arbore, A. Galvanauskas, D. Harter, M. H. Chou, and M. M. Fejer, *Opt. Lett.* **22**, 1341 (1997).
8. M. L. Bortz, M. Fujimura, and M. M. Fejer, *Electron. Lett.* **30**, 34 (1994).
9. K. Mizuuchi, K. Yamamoto, K. Kato, and H. Sato, *IEEE J. Quantum Electron.* **30**, 1596 (1994).
10. Y. Ishigame, T. Suhara, and H. Ishihara, *Opt. Lett.* **3**, 3597 (1991).
11. L. E. Meyers, R. C. Eckardt, M. M. Fejer, R. L. Byer, and W. R. Bosenberg, *Opt. Lett.* **21**, 591 (1996).
12. P. E. Powers, T. J. Kulp, and S. E. Bisson, *Opt. Lett.* **23**, 159 (1998).
13. J. A. Armstrong, N. Bloembergen, and P. S. Pershan, *Phys. Rev.* **127**, 1918 (1962).
14. R. C. Eckardt and J. Reintjes, *IEEE J. Quantum Electron.* **QE-20**, 1178 (1984).
15. L. E. Meyers, R. C. Eckardt, M. M. Fejer, R. L. Byer, W. R. Bosenberg, and J. W. Pierce, *J. Opt. Soc. Am. B* **12**, 2102 (1995).
16. M. Missey, V. Dominic, L. Myers, R. Eckardt, and C. Littell, in *Advanced Solid State Lasers*, C. R. Pollock and W. R. Bosenberg, eds., Vol. 10 of OSA Trends in Optics and Photonics Series (Optical Society of America, Washington, D.C., 1997), p. 247.